Extreme Mechanics Letters 11 (2017) 37–41

Contents lists available at ScienceDirect

Extreme Mechanics Letters

journal homepage: www.elsevier.com/locate/eml

Stable elastic wave band-gaps of phononic crystals with hyperelastic transformation materials

Yan Liu [b], Zheng Chang [a,*], Xi-Qiao Feng [b]

[a] College of Science, China Agricultural University, Beijing, 100083, China

[b] Institute of Biomechanics and Medical Engineering, AML, Department of Engineering Mechanics, Tsinghua University, Beijing 100084, China

ARTICLE INFO

Article history:
Received 17 October 2016
Received in revised form
12 November 2016
Accepted 13 November 2016
Available online 23 November 2016

Keywords:
Phononic crystals
Wave
Hyperelasticity
Transformation
Band-gap

ABSTRACT

The elastic wave band structure in a phononic crystal (PC) is usually affected by the deformations in its soft constituent phase. In this work, hyperelastic transformation materials are proposed in the design of PCs in order to achieve stable elastic band-gaps that do not vary with deformation. It is demonstrated that one-dimensional PCs with a semi-linear soft phase can keep all elastic wave modes unchanged with respect to external deformations. However, only S-wave modes can be precisely retained in the PCs made of a neo-Hookean soft material. The theoretical results and the robustness of the proposed PCs are validated by numerical simulations.

1. Introduction

Phononic crystals (PCs) [1,2] have found a diversity of technologically significant applications. In particular, they have been used in, for instance, filters [3], waveguides [4,5], and sensors [6] to manipulate acoustic and elastic waves. The phononic band structure and dispersion relations can be tailored with appropriate choice of either geometrical/material properties [7–9] or external stimuli [10–12]. In this sense, soft materials play an important role in the performance of PCs. For example, rubbery materials can be utilized to enhance the resonance effect of locally resonant sonic crystals [9]. In recent years, the applications of soft materials in PCs have attracted much attention due to their high sensitivity to deformations [13] and their ability of reversible structural instability [14,15]. These essential features of soft materials open a promising route to realizing PC devices with tunable band-gaps [16,17].

In many applications, stable band-gaps that do not vary with external stimuli are required in the PCs serving in harsh environments with, for instance, large structural deformations and vibrations. The design of such PCs is a challenging issue because soft materials may lose the aforementioned advantages in some harsh circumstances.

Recently, the hyperelastic transformation theory [18–20] has been proposed as a new tool to manipulate elastic waves. Importantly, this theory reveals that hyperelastic transformation media, such as semi-linear materials [18] and neo-Hookean materials [19,20] can behave like smart transformation metamaterials [21] and possess a space invariance in wave applications. These properties shed light on the possibility to design PCs with soft components that have stable band-gaps under external mechanical stimuli.

In this Letter, by invoking the hyperelastic transformation theory, we investigate the band-gap structures of PCs with a hyperelastic transformation medium as the soft component. Considering two classes of typical hyperelastic media—semi-linear materials and neo-Hookean materials, we propose a type of one-dimensional (1D) PCs that manifests unique or partial unique band structures under finite deformations in their soft components. The performance of such PCs serving in a more realistic situation is analyzed, in which the soft component is subjected to random mechanical deformation with varying magnitudes. Both theoretical analysis and numerical simulations demonstrate the robustness of band structures in the proposed PCs.

2. Phononic crystals with hyperelastic transformation material

Consider a 1D layered structure in which a stiff and linear elastic material (A) and a soft hyperelastic material (B) are arranged alternately along the x direction, as shown in Fig. 1(a). In the initial

* Corresponding author.
E-mail address: changzh@cau.edu.cn (Z. Chang).

http://dx.doi.org/10.1016/j.eml.2016.11.007
2352-4316/

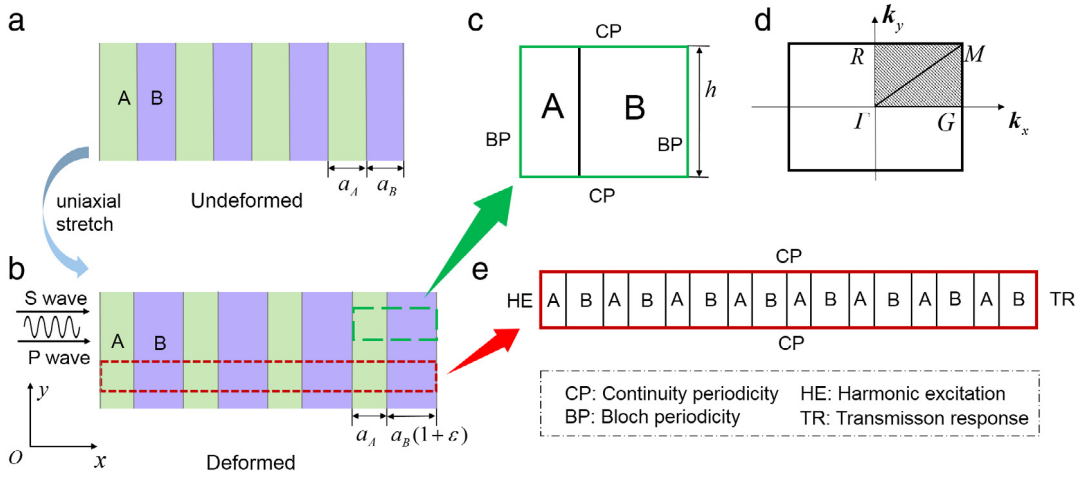

Fig. 1. Schematic diagram of the proposed PC. (a) Initial configuration, and (b) deformed configuration of the PC. The soft component is subjected to uniaxial stretch with the elongation strain ε in the x direction. The P- and S-waves propagate in the x direction. (c) A primitive cell of the PC for predicting the elastic band structures. (d) First Brillouin zone for the primitive cell. The band structure in the reciprocal lattice vector space ($\mathbf{k_x}$, $\mathbf{k_y}$) is considered. (e) A super cell consisting of eight primitive cells for the transmission spectrum analysis of the PC.

configuration, each stiff layer and soft layer have the thicknesses of a_A and a_B, respectively. The stiffness of the stiff layers is much higher than that of the soft ones such that band-gaps with a considerable width can be created. Therefore, we neglect the deformations in the stiff layers and the externally applied deformations are fully undertook by the soft layers. For simplicity, assume that the device is subjected to only uniaxial tension or compression in the x direction, as shown in Fig. 1(b).

The small-on-large theory [22] is utilized to describe the linear elastic wave motion in the hyperelastic material. The governing equation of elastic wave motion reads

$$\nabla \cdot (\mathbf{C} : \nabla \mathbf{u}) = \rho \mathbf{u}_{tt}, \tag{1}$$

where $\mathbf{u}$ is the displacement vector, $\mathbf{C}$ and ρ are the fourth-order tangent stiffness tensor and the effective mass density, respectively. $\mathbf{C}$ and ρ are expressed as

$$C_{ijkl} = J^{-1} F_{i\alpha} F_{k\beta} C_{0\alpha j\beta l}, \qquad \rho = J^{-1}\rho_0, \tag{2}$$

where F_{ij} are the components of the deformation gradient tensor $\mathbf{F}$, $J = \det(\mathbf{F})$, $\mathbf{C_0}$ and ρ_0 are the initial tangent stiffness tensor and the initial mass density, respectively. $\mathbf{C}_0$ can be determined by [22]

$$\mathbf{C_0} = \frac{\partial^2 W}{\partial \mathbf{F} \partial \mathbf{F}}, \tag{3}$$

where W is the strain energy function of the soft material.

First, we assume that the strain energy function W in the soft component has a semi-linear form [18]

$$W = \frac{\lambda_0}{2}(i_1 - 3)^2 + \mu_0\left[(i_1 - 1)^2 - 2i_2 + 2\right], \tag{4}$$

where $i_1 = U_{ii}$ and $i_2 = \frac{1}{2}(U_{ii}U_{jj} - U_{ij}U_{ji})$ are two invariants of the tensor $\mathbf{U} = \left(\mathbf{F}^{\mathbf{T}} \cdot \mathbf{F}\right)^{1/2}$, λ_0 and μ_0 are the initial Lamé constants of the material. According to the hyperelastic transformation theory [18], the semi-linear strain energy function manifests an analogy between the pushing forward operation (Eq. (2)) in the small-on-large theory and the asymmetric transformation relations [23] in the traditional elastodynamic transformation theory [24] when its deformation is free of rotation. This means that the wave responses of the deformed PC shown in Fig. 1(b) will be the same as its initial configuration in Fig. 1(a). In other words, the band structure of the PC is stable and does not vary with the applied deformation.

In the second situation, we assume that the hyperelastic material obeys the neo-Hookean constitutive relation. Its strain energy function is [20]

$$W = \frac{\lambda_0}{2}(J - 1)^2 - \mu_0 \ln J + \frac{\mu_0}{2}(I_1 - 3), \tag{5}$$

where $I_1 = G_{ii}$ is the first invariant of the right Cauchy–Green tensor $\mathbf{G} = \mathbf{F}^{\mathbf{T}} \cdot \mathbf{F}$. For the neo-Hookean material expressed in Eq. (5), however, the analogy between the pushing forward relation and the asymmetric transformation relation holds only for S-waves [20]. Therefore, we cannot obtain a unique band structure by using the neo-Hookean soft component. Nevertheless, all S-wave modes in the band structure can be expected to be identical between the deformed configuration and the initial configuration of the PC.

3. Numerical simulations

To validate the theoretical prediction in Section 2, we perform numerical simulations by using the software COMSOL Multiphysics. A two-step model [20] is adopted to calculate the small-on-large wave motion. The first step is to calculate a static equilibrium equation for the hyperelastic material and to deduce the corresponding effective material parameter in the deformed configuration. The second step is to determine the band structure of the PC by using a weak-form PDE model.

We define a primitive cell in the deformed configuration in order to implement the scheme proposed above, as shown in Fig. 1(c). The initial thicknesses of each stiff layer and soft layer are both set to be $a_A = a_B = 0.01$ m, while the height of the primitive cell is taken as $h = 0.02$ m. In consistency with the above theoretical model, external deformations are only applied to the soft layers. The small deformation in the stiff layers derived from stress continuity is neglected because of the large modulus ratio between the stiff and the soft phases. Periodic boundary conditions are imposed at the four boundaries of the primitive cell. The left and right boundaries of the cell are set to be Bloch periodicity, while the upper and lower boundaries are specified to be continuity periodicity. The band structure on the segment Γ–G of the reciprocal lattice vector space is calculated, as shown in Fig. 1(d).

For example, aluminum and vulcanization rubber are used as the stiff and the soft materials, respectively. Their mechanical parameters are $\rho_A = 2730$ kg/m^3, $\lambda_A = 7.76 \times 10^{10}$ Pa, $\mu_A =$

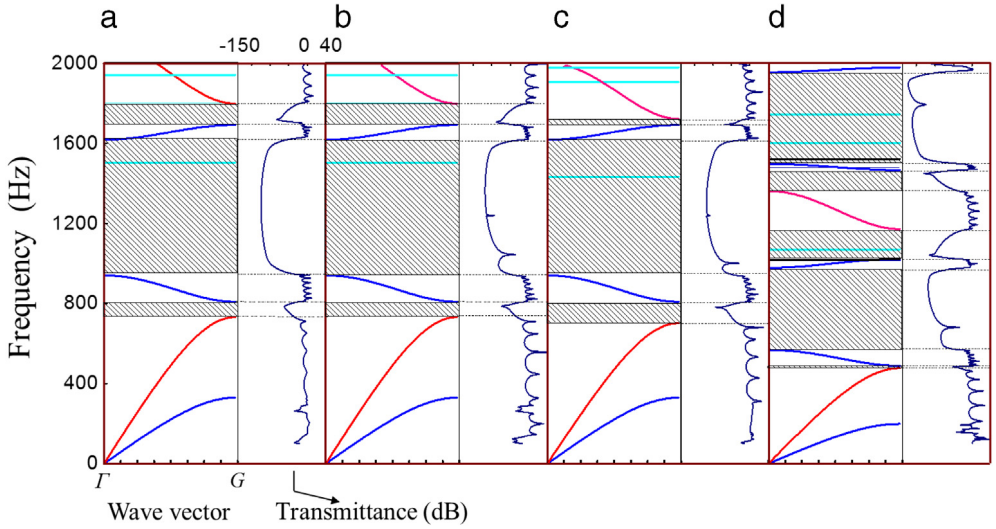

Fig. 2. Band structures (left panel) and transmission spectra (right panel) of the PCs with different soft components. (a) Initial configuration without external deformation in the soft component, which is equivalent to a linear elastic material with initial mechanical parameters. The results obtained by using the (b) semi-linear, (c) neo-Hookean, and (d) Gent hyperelastic models. In (b)–(d), the soft component is subjected to uniaxial stretch with strain $\lambda = 0.3$. In the band structures, the P- and S-modes are distinguished by red and blue curves, respectively, the mixed modes are denoted by cyan curves, and the band-gaps are denoted by the shaded areas. (For interpretation of the references to color in this figure legend, the reader is referred to the web version of this article.)

2.87×10^{10} Pa; $\rho_B = 1300$ kg/m^3, $\lambda_B = 1 \times 10^6$ Pa, and $\mu_B = 3.4 \times 10^5$ Pa. As aforementioned, the semi-linear constitutive relation and the neo-Hookean constitutive relation can be assumed to describe the soft material. For further comparison, we also use the following Gent strain energy function for the soft component:

$$W = -\frac{\mu_0}{2} J_m \log\left(1 - \frac{I_1 - 3}{J_m}\right) - \mu_0 \log J + \left(\frac{\lambda_0}{2} - \frac{\mu}{J_m}\right)(J-1)^2, \tag{6}$$

where J_m is a dimensionless parameter related to the strain saturation of the material. Here we choose $J_m = 0.5$ in accordance with a previous Ref. [13].

Using the semi-linear, neo-Hookean, and Gent models, the band structures of the PC are determined, as shown in Fig. 2. First, we calculate the band structure of the initial configuration in Fig. 1(a), as shown in Fig. 2(a). The P- and S-wave modes are distinguished by the red and blue lines, respectively. Three band-gaps can be observed in the range of [0–2000] Hz, namely [732–808] Hz, [914–1617] Hz, and [1691–1801] Hz, which are independent of the adopted constitutive relations for the soft phase.

In the deformed configuration of the PC, we assume that the soft material is subjected to uniaxial stretch with the elongation strain $\varepsilon = 30\%$. Comparing Fig. 2(a) and (b) shows that when the semi-linear constitutive model is used, the band structure of the deformed PC is exactly the same as that of its initial, undeformed configuration. This conclusion is consistent with our theoretical prediction.

If the soft material obeys the neo-Hookean model, the S-modes (blue lines) of the deformed PC are retained, in consistency with our theoretical prediction. However, the P-modes (red lines) are altered due to the external deformation, as shown in Fig. 2(c). In this sense, the second band-gap keeps unchanged with deformation since its two boundaries are both dictated by the S-modes. The first and the third band-gaps shift from [732–808] Hz and [1691–1801] Hz to [701–808] Hz and [1691–1721] Hz, respectively.

As can be seen from Fig. 2(d), the PC with a Gent component exhibits a totally different band structure, and all band-gaps shift to lower frequencies. Simultaneously, the bandwidths also manifest significant changes. The first band-gap is almost closed, the second band-gap is narrowed by 42%, while the third band-gap is magnified by 56%.

In order to testify the above results, the transmission spectra are also simulated for these examples. In the numerical processes, a super cell with eight primitive cells in the x direction is simulated, as shown in Fig. 1(d). Instead of Bloch periodical boundary conditions, the left boundary of the super cell is set to be a harmonic wave source, while the right boundary is set to be an output terminal. The transmission coefficient, also referred to as transmittance, is defined as $T = 20\log_{10}(u_{out}/u_{in})$, with u_{in} and u_{out} being the integrated displacements on the input and the output terminals, respectively. It is seen from the numerical results in Fig. 2 that the transmission spectra demonstrate a good agreement with the band structures for both the pass bands and band-gaps.

To further examine the influence of deformations on the band structure of a PC with a semi-linear or neo-Hookean component, we simulate the transformation of the band-gaps with increasing uniaxial tension. For the PC with a semi-linear component, all bands keep unchanged even when the applied uniaxial tension is very large. For the neo-Hookean case, all S-modes are independent of uniaxial tension, as demonstrated in Fig. 3. However, the first P-wave mode shifts to a lower frequency, leading to an increase in the first band-gap width for ∼49% when $\varepsilon = 40\%$; the width of the third band-gap reduces with deformation and it is nearly closed at $\varepsilon = 40\%$.

Finally, we consider a more realistic situation by using the transmission spectrum method. Assume that the soft component in the PC is subjected to randomly mechanical deformation in the range of $\varepsilon \in [0\%, 30\%]$. In the super cell defined in Fig. 1(d), different uniaxial stretches are applied to the different soft layers. Three random load distributions are compared, as shown in Fig. 4(a). For the PC with a semi-linear component, the transmission spectra in the three cases totally coincide with each other and are the same as that in the undeformed configuration of the PC. For the PCs with a neo-Hookean component, all boundaries governed by the S-bands, including the higher-frequency boundary of the first band-gap, the two boundaries of the second band-gap, and the lower-frequency boundary of the third band-gap, show no difference in the three loading conditions.

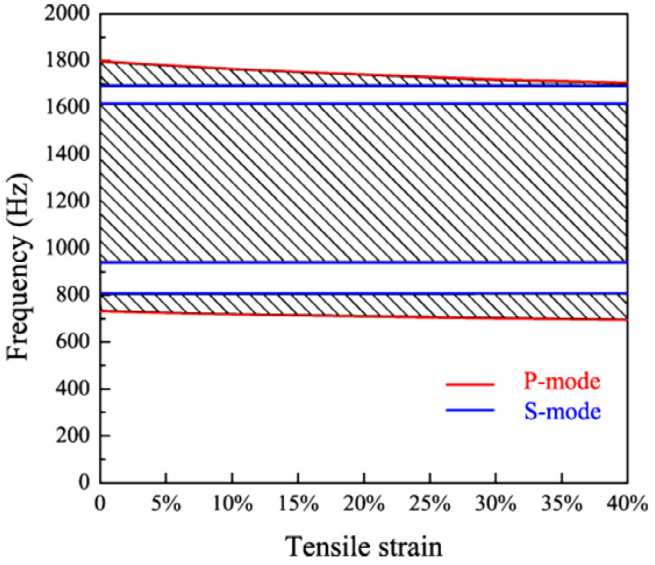

Fig. 3. Variations in the elastic band-gaps of the PC with respect to the tensile strain applied to its neo-Hookean component. The band-gaps are denoted by the shaded areas, and the band-gap boundaries governed by P- and S-modes are distinguished by red and blue color, respectively. (For interpretation of the references to color in this figure legend, the reader is referred to the web version of this article.)

The remaining two band-gap boundaries, though dependent of the loads, vary in a very narrow range of frequency. The shaded areas in Fig. 4(b) demonstrates the band-gaps calculated by averaging the global deformation of the super cell. The good agreement among the transmission spectra (curves) and the band-gap areas (shaded area) demonstrates that the band-gaps of a PC with a neo-Hookean component can be well predicted by averaging its overall deformation. Moreover, the results also illustrate that stable band-gaps can also be expected in the circumstance with random loads.

4. Discussions

The above theoretical and numerical analyses show that semi-linear materials exhibit distinct merits in the design of PCs with stable band-gaps. However, few materials in nature possess a semi-linear soft constitutive relation of relatively large deformation, and the spatial equivalence condition requires that the semi-linear material in the PC undergoes only rotation-free deformations in order to guarantee the stability of its band-gaps [18]. These issues make it very tough to practically realize PCs with stable band-gaps by using semi-linear materials.

In contrary, neo-Hookean materials widely exist in nature. Although a PC made of a neo-Hookean material only has stable S-wave modes, its spatial equivalence is independent of deformations [20]. Our analysis demonstrates that though its third band-gap may be closed under large deformations, the width of the first band-gap can be enlarged by external deformation (Fig. 3). In addition, the PCs made of a neo-Hookean material can exhibit a robustness of performance even when subjected to random mechanical loads (Fig. 4). Therefore, neo-Hookean materials should be a potential candidate to realize PC devices with stable band structures.

5. Conclusions

We have integrated the hyperelastic transformation theory in the design of PCs with stable band structures that do not vary with external deformations. It is demonstrated, both theoretically

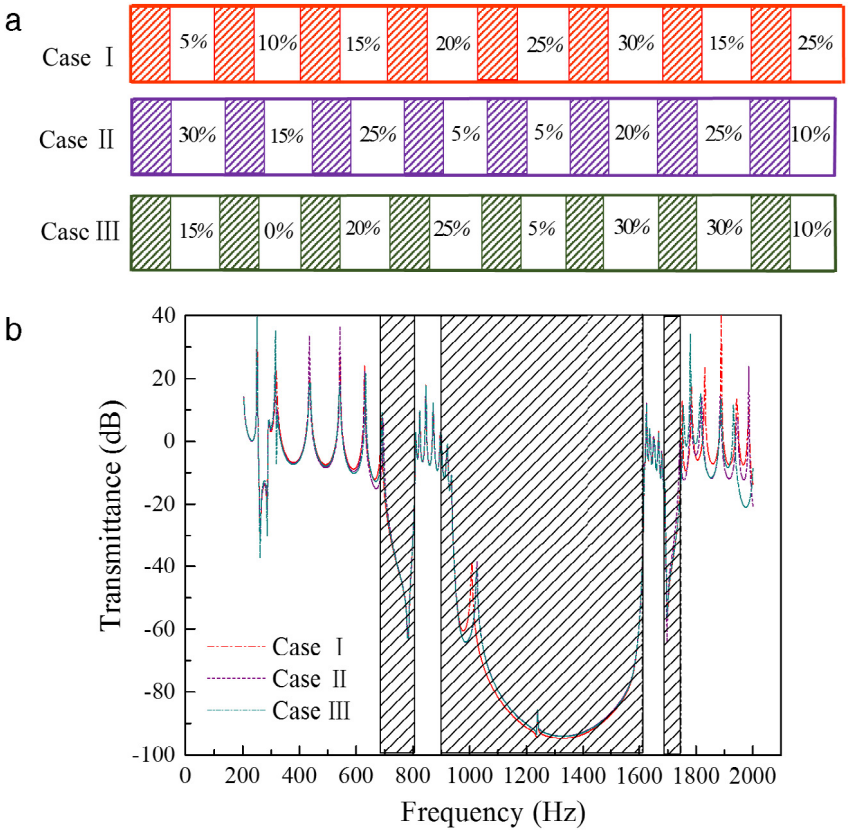

Fig. 4. Transmission spectra of a PC with a neo-Hookean soft component subjected to randomly distributed deformations. (a) Three different distributions of random tensile strains applied to the different layers of the soft component, and (b) the corresponding transmission spectra. The shaded areas denote the band-gaps obtained from the simulations of the super cell.

and numerically, that the band structure of a 1D PC made of a semi-linear material will keep unchanged with deformation. For a PC made of a neo-Hookean medium, deformations do not affect its S-modes but have significant effects on the P- modes. The analysis of the band-gap transformation shows that neo-Hookean materials can be utilized to realize PCs with stable band-gaps. The proposed PCs may can be applied in some fields where high precision transmission and measurement are required. This work also provide inspirations for the design of elastodynamic cloaks [18,19], elastic wave mode splitters [20], shear wave beam bands [25], and impact-tolerant composites.

Acknowledgment

This work was supported by the National Natural Science Foundation of China (Grant Nos. 11432008 and 11602294).

References

[1] M. Sigalas, E. Economou, Elastic and acoustic wave band structure, J. Sound Vib. 158 (1992) 377–382.
[2] M.S. Kushwaha, P. Halevi, L. Dobrzynski, B. Djafari-Rouhani, Acoustic band structure of periodic elastic composites, Phys. Rev. Lett. 71 (1993) 2022–2025.
[3] Y. Pennec, B. Djafari-Rouhani, J. Vasseur, A. Khelif, P. Deymier, Tunable filtering and demultiplexing in phononic crystals with hollow cylinders, Phys. Rev. E 69 (2004) 046608.
[4] M. Kafesaki, M. Sigalas, N. Garcia, Frequency modulation in the transmittivity of wave guides in elastic-wave band-gap materials, Phys. Rev. Lett. 85 (2000) 4044–4047.
[5] J.H. Sun, T.T. Wu, Propagation of acoustic waves in phononic-crystal plates and waveguides using a finite-difference time-domain method, Phys. Rev. B 76 (2007) 104304.
[6] R. Lucklum, J. Li, Phononic crystals for liquid sensor applications, Meas. Sci. Technol. 20 (2009) 124014.
[7] T.T. Wu, Z.G. Huang, S. Lin, Surface and bulk acoustic waves in two-dimensional phononic crystal consisting of materials with general anisotropy, Phys. Rev. B 69 (2004) 094301.
[8] X. Zhang, Z. Liu, Y. Liu, F. Wu, Elastic wave band gaps for three-dimensional phononic crystals with two structural units, Phys. Lett. A 313 (2003) 455–460.
[9] Z. Liu, X. Zhang, Y. Mao, Y.Y. Zhu, Z. Yang, C.T. Chan, P. Sheng, Locally resonant sonic materials, Science 289 (2000) 1734–1736.
[10] J. Vasseur, O.B. Matar, J. Robillard, A.C. Hladky-Hennion, P.A. Deymier, Band structures tunability of bulk 2D phononic crystals made of magneto-elastic Materials, AIP Adv. 1 (2011) 041904.
[11] X.Y. Zou, Q. Chen, B. Liang, J.C. Cheng, Control of the elastic wave bandgaps in two-dimensional piezoelectric periodic structures, Smart Mater. Struct. 17 (2007) 015008.
[12] K. Bertoldi, M. Boyce, Mechanically triggered transformations of phononic band gaps in periodic elastomeric structures, Phys. Rev. B 77 (2008) 052105.
[13] K. Bertoldi, M.C. Boyce, Wave propagation and instabilities in monolithic and periodically structured elastomeric materials undergoing large deformations, Phys. Rev. B 78 (2008) 184107.
[14] D. Yang, L. Jin, R.V. Martinez, K. Bertoldi, G.M. Whitesides, Z. Suo, Phase-transforming and switchable metamaterials, Extreme Mech. Lett. 6 (2016) 1–9.
[15] B. Li, Y.P. Cao, X.Q. Feng, H. Gao, Mechanics of morphological instabilities and surface wrinkling in soft materials: a review, Soft Matter 8 (2012) 5728–5745.
[16] J. Shim, P. Wang, K. Bertoldi, Harnessing instability-induced pattern transformation to design tunable phononic crystals, Int. J. Solids Struct. 58 (2015) 52–61.
[17] G.Y. Li, Y. Zheng, Y. Cao, X.Q. Feng, W. Zhang, Controlling elastic wave propagation in a soft bilayer system via wrinkling-induced stress patterns, Soft Matter 12 (2016) 4204–4213.
[18] A.N. Norris, W.J. Parnell, Hyperelastic cloaking theory: transformation elasticity with pre-stressed solids, Proc. R. Soc. Lond. Ser. A Math. Phys. Eng. Sci. 468 (2012) 2881–2903.
[19] W.J. Parnell, A.N. Norris, T. Shearer, Employing pre-stress to generate finite cloaks for antiplane elastic waves, Appl. Phys. Lett. 100 (2012) 171907.
[20] Z. Chang, H.Y. Guo, B. Li, X.Q. Feng, Disentangling longitudinal and shear elastic waves by neo-Hookean soft devices, Appl. Phys. Lett. 106 (2015) 161903.
[21] D. Shin, Y. Urzhumov, Y. Jung, G. Kang, S. Baek, M. Choi, H. Park, K. Kim, D.R. Smith, Broadband electromagnetic cloaking with smart metamaterials, Nature Commun. 3 (2012) 542–555.
[22] R.W. Ogden, Incremental statics and dynamics of pre-stressed elastic materials, in: M. Destrade, G. Saccomandi (Eds.), Waves in Nonlinear Pre-Stressed Materials, in: CISM Int. Centre for Mechanical Sciences, vol. 495, Springer, Berlin, 2007, pp. 1–26. (chapter 1).
[23] M. Brun, S. Guenneau, A.B. Movchan, Achieving control of in-plane elastic waves, Appl. Phys. Lett. 94 (2009) 061903.
[24] A.N. Norris, A.L. Shuvalov, Elastic cloaking theory, Wave Motion 48 (2011) 525–538.
[25] Z. Chang, H.Y. Guo, B. Li, X.Q. Feng, Response to Comment on 'Disentangling longitudinal and shear elasticwaves by neo-Hookean soft devices, Appl. Phys. Lett. 107 (2015) 056102.